



The University of
Nottingham

UNITED KINGDOM · CHINA · MALAYSIA

Raouf, Saad M. and Koutas, Lampros N. and Bournas, Dionysios A. (2016) Bond between textile-reinforced mortar (TRM) and concrete substrates: experimental investigation. *Composites Part B: Engineering* . ISSN 1359-8368 (In Press)

Access from the University of Nottingham repository:

<http://eprints.nottingham.ac.uk/33391/1/1-s2.0-S1359836816307041-main.pdf>

Copyright and reuse:

The Nottingham ePrints service makes this work by researchers of the University of Nottingham available open access under the following conditions.

This article is made available under the Creative Commons Attribution licence and may be reused according to the conditions of the licence. For more details see:
<http://creativecommons.org/licenses/by/2.5/>

A note on versions:

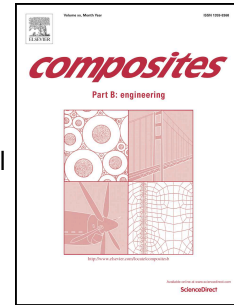
The version presented here may differ from the published version or from the version of record. If you wish to cite this item you are advised to consult the publisher's version. Please see the repository url above for details on accessing the published version and note that access may require a subscription.

For more information, please contact eprints@nottingham.ac.uk

Accepted Manuscript

Bond between textile-reinforced mortar (TRM) and concrete substrates: Experimental investigation

Saad M. Raouf, Lampros N. Koutas, Dionysios A. Bournas



PII: S1359-8368(16)30704-1

DOI: [10.1016/j.compositesb.2016.05.041](https://doi.org/10.1016/j.compositesb.2016.05.041)

Reference: JCOMB 4324

To appear in: *Composites Part B*

Received Date: 18 February 2016

Revised Date: 30 April 2016

Accepted Date: 15 May 2016

Please cite this article as: Raouf SM, Koutas LN, Bournas DA, Bond between textile-reinforced mortar (TRM) and concrete substrates: Experimental investigation, *Composites Part B* (2016), doi: 10.1016/j.compositesb.2016.05.041.

This is a PDF file of an unedited manuscript that has been accepted for publication. As a service to our customers we are providing this early version of the manuscript. The manuscript will undergo copyediting, typesetting, and review of the resulting proof before it is published in its final form. Please note that during the production process errors may be discovered which could affect the content, and all legal disclaimers that apply to the journal pertain.

Bond between Textile-Reinforced Mortar (TRM) and Concrete Substrates: Experimental Investigation

Saad M. Raouf^{a,b,*}, Lampros N. Koutas^a, Dionysios A. Bournas^c

^a Department of Civil Engineering, University of Nottingham, NG7 2RD, Nottingham, UK

^b Department of Civil Engineering, Tikrit University, Iraq- Tikrit

^c European Commission, Joint Research Centre (JRC), Institute for the Protection and Security of the Citizen (IPSC), European Laboratory for Structural Assessment, TP480, via Enrico Fermi 2749, I-21020 Ispra (VA), Italy.

*Corresponding author. Tel.: +44 (0) 7741830587. E-mail: evxsmr@nottingham.ac.uk

Abstract:

This paper presents an extended experimental study on the bond behaviour between textile-reinforced mortar (TRM) and concrete substrates. The parameters examined include: (a) the bond length (from 50 mm to 450 mm); (b) the number of TRM layers (from one to four); (c) the concrete surface preparation (grinding versus sandblasting); (d) the concrete compressive strength (15 MPa or 30 MPa); (e) the textile coating; and (f) the anchorage through wrapping with TRM jackets. For this purpose, a total of 80 specimens were fabricated and tested under double-lap direct shear. It is mainly concluded that: (a) after a certain bond length (between 200 mm and 300 mm for any number of layers) the bond strength marginally increases; (b) by increasing the number of layers the bond capacity increases in a non-proportional way, whereas the failure mode is altered; (c) concrete sandblasting is equivalent to grinding in terms of bond capacity and failure mode; (d) concrete compressive strength has a marginal effect on the bond capacity; (e) the use of coated textiles alters the failure mode and significantly increases the bond strength; and (f) anchorage of TRM through wrapping with TRM jackets substantially increases the ultimate load capacity.

Keywords: A. Fabrics/textiles; A. Carbon fibre; B. Debonding; C. Mechanical testing; Concrete strengthening.

30 **1 Introduction and background**

31 The need for retrofitting the existing concrete infrastructure is progressively becoming more
32 important due to their continuous deterioration as a result of ageing, environmental induced
33 degradation, lack of maintenance or need to meet the current design requirements (i.e.
34 Eurocodes). Replacing the deficient concrete structures in the near future with new is not a
35 viable option as it would be prohibitively expensive. For this reason a shift from new
36 construction towards renovation and modernization has been witnessed in the European
37 construction sector, between 2004 and 2013, with practically 50% of the total construction
38 output being renovation and structural rehabilitation. (i.e. €305bn turnover on rehabilitation
39 and maintenance works in EU27 for 2012, see www.fiec.eu).

40 The use of externally bonded (EB) composite materials (such as fiber reinforced
41 polymers - FRPs) is a common retrofitting technique usually employed by engineers. Almost
42 a decade ago, an innovative cement-based composite material, the so-called textile-reinforced
43 mortar (TRM), was introduced in the field of structural retrofitting [1, 2] as an alternative to
44 FRP solution, addressing cost and durability issues. Since then, TRM progressively attracts
45 the interest of the structural engineering community.

46 TRM comprises high-strength fibers (i.e. carbon, glass or basalt) in form of textiles
47 combined with inorganic matrices (such as cement-based mortars). The textiles that are used
48 as reinforcement of the composite material typically comprise fiber rovings in two orthogonal
49 directions, thus creating open-mesh geometry. TRM is an attractive retrofitting solution
50 because it combines the outstanding properties of composite materials (e.g. high-strength,
51 low weight, corrosion resistance) with the favourable characteristics offered by mortars and
52 cannot be found in resins (e.g. fire resistance, low cost, ability to apply on wet surfaces and
53 low temperatures, air permeability of the substrate. The same material is also referred in the
54 literature as fabric-reinforced cementitious matrix (FRCM) (e.g. [3]).

55 Significant research effort has been put in the last decade to exploit TRM in several
56 cases of retrofitting reinforced concrete (RC) structures; namely flexural [i.e. 4-7], shear
57 strengthening of RC elements [i.e. 8-11], confinement of RC columns [i.e. 1, 2]), seismic
58 retrofitting of RC columns (e.g. [2, 12-16]), seismic retrofitting of infilled RC frames [17].
59 TRM has also been successfully used for retrofitting masonry structures (e.g. out-of-plane
60 strengthening [18] and shear strengthening of masonry walls [19]). However the number of
61 studies on the bond behaviour between TRM and concrete are relatively limited [20-27]. The
62 study of the bond behaviour between TRM and concrete is of crucial importance as it helps
63 understanding the complex mechanisms of transferring forces from the textile reinforcement
64 to the surrounding matrix and eventually to the concrete substrate. It is also a fundamental
65 step towards the development of design models to be used in strengthening applications.

66 Past studies on the bond between TRM and concrete were mainly focused on the
67 behaviour of textiles comprising polyparaphenylene benzobisoxazole (PBO) fibers, except
68 for those in [21, 23] where uncoated carbon and glass fibers [21] and coated carbon fibers
69 [23] were used. With the maximum number of TRM layers investigated being equal to two,
70 the common conclusion of past studies was that for bond lengths varying from 50 mm to 450
71 mm, failure occurs within the composite material, namely at the interface between the fibers
72 and the surrounding mortar. This failure mode typically includes slippage of the fibers within
73 the mortar and is usually described as debonding at fibers/matrix interface. Failure at the
74 interface between the mortar and concrete substrate without involving though any part of the
75 concrete cover was very rarely reported [25, 26]. Ombres [26] attributed the alteration of the
76 failure mode to the increase of the number of layers from one to two. Other parameters, such
77 as the concrete compressive strength and the surface preparation, have been investigated only
78 in [25] and it was found to have insignificant effect on the bond capacity of one PBO-TRM
79 layer bonded to concrete.

80 From the literature survey it becomes clear that the subject of the bond behaviour
81 between TRM and concrete has not sufficiently been covered. In this paper the authors
82 investigate for the first time systematically a set of parameters, focusing on the load response
83 and the failure modes of the EB TRM reinforcement, namely:

- 84 • the number of TRM layers, from one to four, which is beyond the current limit of two,
- 85 • the bond length, from 50 mm to 450 mm,
- 86 • the concrete surface preparation,
- 87 • the concrete compressive strength,
- 88 • the coating of the textile, which has not been investigated before in comparison with
89 uncoated textiles, and
- 90 • the anchorage through wrapping with TRM jackets, which again is a parameter not
91 previously investigated.

92 In addition, the textile used in this study comprises carbon fibers, which are commonly
93 used in strengthening applications. Details are provided in the following sections.

94 **2 Experimental programme**

95 **2.1 Test Specimens and experimental parameters**

96 The main objective of this study was to investigate the bond between TRM and
97 concrete considering different parameters. A total of 80 specimens were fabricated and tested
98 under double-lap direct shear. The geometry of the specimens is shown in Fig. 1. Each
99 specimen comprised two 100 mm-square-section RC prisms connected only by TRM layers
100 bonded on two opposite sides of the prisms. The length of the prisms was equal to 250 mm in
101 all cases, except from two prisms that were constructed 500 mm long for examining a bond
102 length of 450 mm. The bond width of TRM was the same for all the specimens and equal to
103 80 mm. Both prisms were reinforced with steel cages as illustrated in Fig. 1b.

104 The key investigated parameters of this study comprised:

- 105 a) the bond length;
- 106 b) the number of TRM layers;
- 107 c) the concrete surface preparation;
- 108 d) the concrete compressive strength;
- 109 e) the coating of the textile; and
- 110 f) the anchorage through wrapping with TRM jackets.

111 The 80 specimens comprised 40 twin specimens as a measure to reduce the scatter of
112 the results. Parameters (a) and (b) were examined on 22 twin specimens (44 specimens in
113 total), with the bond length varying from 50 to 450 mm and the number of layers from one to
114 four. Six twin specimens were tested to investigate parameter (c), namely the effect of the
115 concrete surface preparation (grinding or sandblasting), whereas other six twin specimens
116 were used to evaluate the effect of the concrete compressive strength (15 or 30 MPa) on the
117 results [parameter (d)]. Four twin specimens were tested to examine the influence textile
118 coating on the ultimate load and failure mode [parameter (e)], and two twin specimens were
119 used to investigate the effect of anchorage through wrapping with TRM jackets [parameter
120 (f)].

121 The notation of specimens addressing parameters (a) and (b) was LX_N, where X is the
122 bond length and N is the number of TRM layers. For the other specimens, the notation was
123 LX_N_Y, with Y denoting the investigated parameter: S for concrete surface preparation; Ls
124 for low concrete compressive strength; C for coated textile and W for TRM wrapping. Details
125 of the different strengthening configurations and number of tested specimens for each
126 parameter are listed in Table 1.

127 **2.2 Materials and strengthening procedure**

128 The RC prisms were cast in different groups and dates. For all tested specimens, the targeted
129 concrete compressive strength was 30 MPa, except for group LN_X_Ls (twelve specimens)
130 where the targeted compressive strength was lower and equal to 15 MPa. The compressive
131 strength of all specimens was measured on the day of the testing (average value of three
132 150x150x150 mm cubes) and is given in Table 1.

133 The strengthening system applied in this study comprised high-tensile strength carbon
134 fiber textile embedded into cement-based mortar. The textile had equal quantity of carbon
135 fibers in the two orthogonal directions with a mesh of 10 mm (Fig. 2). The weight of the
136 carbon textile reinforcement was 348 g/m², whereas its nominal thickness (based on the
137 equivalent smeared distribution of fibers) was 0.095 mm. According to the manufacturer
138 datasheets, the tensile strength and modulus of elasticity of the carbon fibers were 3800 MPa
139 and 225 GPa, respectively. The matrix consisted of an inorganic dry mortar comprising
140 cement and polymers at a ratio of 8:1 by weight. The water-binder ratio of the mortar was
141 0.23:1 by weight, resulting in plastic consistency and good workability. The compressive and
142 flexural strength of the mortar (average value from 3 prisms) were experimentally obtained
143 on the day of testing using prisms with dimensions of 40x40x160 mm according to EN 1015-
144 22 [28] and are given in Table 1.

145 The concrete surface was prepared prior to strengthening by removing a thin layer of
146 concrete (with the use of a grinder) and creating a grid of groves (with a depth of
147 approximately 3 mm - Fig. 3a). This procedure was followed for all specimens, except for
148 those of group LX_N_S, where the concrete surface was sandblasted (Fig. 3b). After cleaning
149 and dampening the concrete surface, the first layer of mortar with approximately 2 mm
150 thickness was placed on the concrete surface using a metallic trowel (Fig. 4a). Then the first
151 textile layer was applied and pressed slightly into the mortar, which protruded through the
152 perforations between the fiber rovings as shown in Fig. 4b. This procedure was repeated until

153 the required number of TRM layers was applied. Finally, an external layer of mortar with
154 approximately 3 mm thickness was applied and levelled by trowel (Fig. 4c). Of crucial
155 importance in this method was the application of each mortar layer while the previous one
156 was still in a fresh state.

157 For the specimens retrofitted with coated textile (LX_N_C), an epoxy resin was used.
158 The adhesive used for the coating was a low viscosity, two-part epoxy resin. The tensile
159 strength and the elastic modulus of this adhesive were equal to 72.4 MPa and 3.18 GPa,
160 respectively (taken from the manufacturer data sheets).

161 For the specimens received wrapping, namely the longitudinal TRM composite was
162 anchored through TRM jackets wrapped around the concrete prism (group LX_N_W),
163 additional surface preparation was made prior to strengthening including rounding of the
164 prism corners to a radius of 10 mm. After applying the required number of longitudinal TRM
165 layers, the prism side under investigation was wrapped with two TRM layers following the
166 strengthening procedure previously described. The width of the textile used for wrapping was
167 100 mm which was equal to the bond length of the longitudinal TRM layers (Fig. 4d).

168

169 **2.3 Experimental setup and procedure**

170 All specimens were tested after a curing period of six weeks (same curing conditions were
171 applied to all specimens). The experimental setup included two steel clamps which were
172 fixed at one side (restrained side) of the specimen to ensure that failure would occur in the
173 monitored side (Fig. 1a and Fig. 5). The TRM composite was left un-bonded at a 100 mm-
174 long central zone (50 mm at each prism) of the specimen (Fig. 1a) to prevent concrete-edge
175 failure which could have adverse effects. All tests were carried out using a universal tensile
176 testing machine of 250 kN capacity. The specimens were gripped to the tensile machine using
177 the 16 mm steel bars fitted at the centre of each prism during casting (these bars were

178 terminated at the interface between the two prisms- Fig. 6a). To ensure full alignment
179 between the two prisms, two 10 mm diameter acrylic dowels were inserted into the concrete
180 mass of the prisms (fig. 6b) (after casting and prior to the strengthening application) at pre-
181 made holes (Fig. 6a). The load was applied at a displacement control with rate of 0.2
182 mm/min. Two LVDTs were mounted to the unstrengthened sides of the specimens to record
183 the displacement of the joint (Fig. 5).

184 In a number of previous studies the single-lap shear test set-up was used to investigate
185 the bond of one TRM layer to concrete [21-22, 25-26]. However, the double-lap shear test
186 set-up was selected for this study, which is a modification of the set-up proposed in [29] for
187 testing the bond between FRP composites and concrete. The selection of the double-lap shear
188 test set-up was deemed necessary for testing more than one TRM layers, as with such a set up
189 the stresses are transferred from the concrete to the composite material indirectly, simulating
190 realistically real-world applications. In contrast, in single-lap tests the load is applied directly
191 to the composite material, which means that shear stresses between layers cannot be
192 developed in case of more than one TRM layer.

193

194 **3. Experimental results**

195 Key results of all tested specimens are presented in Table 2 which includes:

196 (1) the maximum load (P_{max}) carried out by the TRM strips for both twin specimens S1 and
197 S2,

198 (2) the displacement (average of two LVDTs readings) which corresponds to the maximum
199 load (δ_{max}),

200 (3) the average load (P_{av}) of the two twin specimens,

201 (4) the average displacement (δ_{av}) of the two twin specimens,

202 (5) the corresponding average normal stress in the textile (σ_t), and

203 (6) the failure mode.

204 The value of normal stress was calculated using Eq. 1:

$$205 \quad \sigma_t = \frac{(P_{av}/2)}{n*t*b} \quad (1)$$

206 Where n is the number of TRM layers, t is the equivalent thickness of the textile in the
207 longitudinal direction ($t=0.095\text{mm}$), and b is the bond width ($b= 80 \text{ mm}$). Equation (1) was
208 used to calculate the normal stress of the fibers excluding the contribution of the mortar. This
209 is typical in the case of TRM systems, and is valid for the ultimate capacity, since the matrix
210 has been cracked. At this load level, all the tension is carried by the textile reinforcement.

211 Starting from the specimens LX_N that were strengthened with one up to four TRM
212 layers at bond lengths of 50, 100, 150, 200 and 250 mm, the maximum load recorded
213 (average from twin specimens) was (see also Table 2): (a) 7.7, 11.6, 12.2, 13.9, and 16.1, kN,
214 respectively, for the specimens with one TRM layer, (b) 18.4, 23.5, 25.3, 28.1, and 29.4kN,
215 respectively, for the specimens with two TRM layers, (c) 22.6, 31.2, 35.1, 36.0, and 38.03
216 kN, respectively, for the specimens with three TRM layers, and (d) 27.9, 35.0, 37.9, 41.5, and
217 41.8 kN, respectively, for the specimens with four TRM layers. The bond length of 450 mm
218 was investigated only for one and two TRM layers, with the corresponding maximum load
219 equal to 17.4 and 31.6 kN, respectively.

220 Figure 7 shows the load-displacement curves (average of the two LVDTs readings)
221 recorded for specimens LX_N. For better illustration, only one of the twin specimens
222 response curve is included, whereas they have been grouped according to the number of
223 TRM layers applied. It is noted that the trend of the curves of twin specimens was similar in
224 all the cases (see “S1” and “S2” columns in Table 2). A common characteristic of all curves
225 is their behaviour up to the maximum load. In specific, a first ascending linear branch with
226 high axial stiffness is followed by a second ascending non-linear branch with progressively
227 decreasing stiffness due to mortar cracking. The post-peak behaviour was different depending

228 on the failure mode which in turn was different depending on the amount of TRM
229 reinforcement. For one and two TRM layers, the post-peak behaviour was generally
230 characterized by a progressive load-drop to a residual strength (Figs 7a and b). In contrast,
231 when three and four TRM layers were applied the load-drop was sudden without any residual
232 strength provided (Figs 7c and d).

233 The failure modes observed in LX_N specimens can be classified in two types: (a)
234 slippage of the fibers within the mortar (Fig. 8a and b), and (b) debonding of TRM from the
235 concrete substrate with peeling off part of the concrete cover (Fig. 8c, d and e). The first
236 failure mode occurred in all specimens with one or two TRM layers, whereas the second
237 occurred in all specimens with three or four layers.

238 For the specimens strengthened with one or two TRM layers, the failure mechanism
239 was controlled by slippage and partial rupture of the longitudinal fibers through the mortar at
240 the loaded end, where a single crack was developed (at an early loading stage) and further
241 opened at the end of the test (Fig. 8a and b). After failure, a residual strength was recorded
242 which was attributed both to the contribution of friction between the inner filaments
243 themselves and the outer filaments with the surrounding matrix.

244 When TRM debonding from the concrete substrate occurred, it was accompanied by
245 removal of a thin concrete cover layer (Fig. 8c, d and e). Failure was initiated by the
246 formation of a longitudinal crack at the loaded end; this crack was continuously propagating
247 towards the free end as the load was increasing. At peak load, propagation of the crack up to
248 free end caused full detachment (debonding) of the TRM composite from the concrete
249 surface and the load dropped to zero. A noticeable difference between the specimens failed
250 due to fibers slippage and those specimens failed due to TRM debonding is that in the latter
251 case several transversal cracks developed on the TRM face as shown in Fig. 9. Hence, a
252 better distribution of stresses along the bond length was achieved in these cases. After

253 debonding occurred, a rotation of the specimen with respect to the longitudinal axes was
254 observed (Fig. 9). This is because the failure was control by one of the two monitored sides
255 of the concrete prism. However, this rotation had no effect on the behaviour up to the
256 ultimate load.

257 Specimens LX_N_S, with different concrete surface preparation (sandblasting instead
258 of grinding), attained maximum loads of 31.2, 33.9 and 40.4 kN for three layers, and 36.1,
259 37.2 and 41.9 kN for four layers, for bond lengths equal 100, 150 and 200 mm, respectively.
260 As illustrated in Fig. 10a, the global behaviour of these specimens (in terms of force-
261 displacement curves) is nearly identical to their counterparts from the LX_N group,
262 indicating that the concrete surface preparation did not affect the bond behaviour. Also the
263 failure mode remained unchanged, comprising TRM debonded from the concrete substrate at
264 the mortar-concrete interface with a thin layer of the concrete cover being peeled-off (Fig.
265 11a).

266 As shown in Table 2, supported by Fig. 10b, specimens with low concrete strength
267 (LX_N_Ls) reached an ultimate load of 29.9, 30.7 and 34.9 kN for three layers, and 32.2,
268 35.1 and 37.7 kN for four layers, for bond lengths of 100, 150 and 200 mm, respectively. As
269 illustrated in Fig. 10b, the global behaviour of this group of specimens was very similar to
270 their counterparts with higher concrete strength in terms of force-displacement curves.
271 Debonding of TRM from the concrete substrate was accompanied with removal of concrete
272 particles which remained attached to the debonded TRM strip (Fig. 11b)

273 The force-displacement curves of the specimens retrofitted with coated textiles
274 (LX_N_C) are presented in Fig. 10c. The ultimate load for one TRM layer was 21.9 kN and
275 23.9 kN for 150 and 200 mm bond length, respectively, which is substantially higher with
276 respect to their counterparts. The corresponding ultimate load for two TRM layers was 29.5
277 and 31.9 kN for 150 and 200 mm bond length, respectively. As shown in Fig. 10c the post-

278 peak behaviour of LX_N_C specimens was different from their counterparts from group
279 LX_N, owing to the different failure mode observed. In particular, all specimens with coated
280 textiles failed due to debonding of TRM at the textile/mortar interface (Fig. 11c), whereas
281 their counterparts failed due to slippage of the textile fibers through the mortar (Figs 8a and
282 b). Failure in this case was within the TRM thickness, and is associated to the stiff behaviour
283 of the coated textiles. This type of failure mode can also be described as inter-laminar
284 shearing. A denser crack pattern was observed in all specimens with the coated textiles,
285 indicating a better activation of the textile fibers in tension.

286 Finally, the load- displacement curves for specimens LX_N_W, which were wrapped
287 with two TRM layers in order to provide better anchorage, are shown in Fig. 12a; Specimens
288 L100_3_W and L100_4_W, reached an ultimate load of 40 and 50.8 kN for three and four
289 layers, respectively (for 100 mm bond length). In terms of ultimate load they performed
290 better than their counterparts (Table 2), whereas a change on the failure mode was also
291 observed. Wrapping of the prism did not allow for debonding of the TRM strips and damage
292 was localized in the loaded-end, where a single transversal crack appeared Fig. 12b.
293 Ultimately, the textile fibers slipped through the mortar resulting in a residual capacity as
294 shown in Fig. 12a.

295 **4. Discussion**

296 In terms of the various parameters investigated in this experimental programme, an
297 examination of the results in terms of ultimate loads and failure modes revealed the following
298 information.

299 4.1 Influence of the bond length and the number of layers

300 The effect of the bond length and the number of layers on the load-carrying capacity is
301 depicted in Fig. 13. The curves in Fig. 13 clearly demonstrate that by increasing either the
302 bond length or the number of layers, the bond capacity increases in a non-proportional way.
303 Similar to the bond behaviour of FRP strips [31], after a certain bond length the anchorage
304 force tends to reach a constant value which is considered as the maximum anchorage force.
305 This length is called “effective bond length” (L_{eff}) and according to the curves provided in
306 Fig. 13 is in the range of 200 and 300 mm for the number of layers (one to four) investigated.
307 This in agreement with the conclusions of previous studies [20, 22-23]. Even in cases with
308 one and two TRM layers, where there is significant friction between the inner and outer
309 filaments when slippage occurs, by providing a large bond length (450 mm) the load capacity
310 was marginally increased.

311 For the same bond length, increasing the number of layers resulted in an increase in the
312 load-carrying capacity. This effect was more pronounced for the transition from one to two
313 layers, whereas for more layers it was gradually becoming less significant. Almost the same
314 trend was followed for all examined bond lengths between 50 and 250 mm. The most
315 important effect of increasing the number of layers though, is related to the change in the
316 failure mode. In particular, as explained in the results section, specimens of LX_N group
317 strengthened with one or two layers failed due to slippage of the textile fibers through the
318 mortar, whereas specimens with three or four layers failed due to TRM debonding from the
319 concrete substrate with peeling off of a part of the concrete cover.

320 The above finding adds new information to the existing knowledge, because in all
321 previous studies on bond between TRM and concrete (where the maximum number of layers
322 examined was two), failure occurred either at the interface between fibers and mortar or at the
323 interface between concrete and mortar without involving the concrete cover. It is noted that

324 failure of TRM involving peeling off of the concrete cover has also been reported in the study
325 of Tetta et al. 2015 [10], where RC beams were retrofitted in shear with TRM U-jackets, and
326 has also been observed by the authors in flexural strengthening of RC beams with TRM [30].
327 This type of failure is very common in case of FRP bonded to concrete [31], indicating that
328 TRMs can behave similar to FRPs.

329 The bond length had also an effect on the residual strength of the specimens failed due
330 to slippage of the fibers, which is related to the friction developed between the inner and the
331 outer filaments of each individual fiber roving. Table 3 shows the percentage of residual load
332 compared to the maximum load recorded for specimens one and two TRM layers. It is
333 generally concluded that the larger the bond length, the higher the slipping surfaces become,
334 so the residual strength do.

335 Figure 14 shows the variation of the normal stress in the textile fibers [calculated by
336 Eq. (1)] with the bond length for different number of TRM layers. It is generally observed
337 that by increasing the number of layers the normal stress decreases, which is consistent with
338 the behaviour of FRP bonded plates to concrete [31]. Only for the transition from one to two
339 layers, the stress in the fibers marginally increases for bond length between 50 and 200 mm.
340 This is possibly connected to the complex mechanism of fibers slippage occurring in
341 specimens with one and two TRM layers.

342

343 **4.2 Influence of surface preparation**

344 Figures 15a and b show a comparison between the ultimate loads of specimens having the
345 same bond length but different concrete surface preparation, for three (Fig. 15a) and four
346 (Fig. 15b) TRM layers. In the majority of the cases, grinding the concrete surface and
347 creating of a grid of grooves is as effective as sandblasting in transferring shear stresses from
348 TRM to concrete. Moreover, the shape of the force-displacement curves in Fig. 10 is the

349 same for both surface preparation methods. Hence, it can be concluded that both ways of
350 surface preparation are suitable, something that needs further investigation for other textile
351 geometries and other types of mortar. This is in agreement with the study of D' Antino et al.
352 2015 [25] where no differences were observed between specimens with untreated and
353 sandblasted concrete surfaces, strengthened with one PBO-fibers TRM layer.

354

355 **4.3 Influence of concrete compressive strength**

356 The concrete compressive strength was selected to be investigated only for three and four
357 TRM layers, because of the failure mechanism observed in LX_N specimens. In particular,
358 TRM debonding from the concrete substrate involving part of the concrete cover (a failure
359 mechanism which is associated to the concrete strength) occurred only in the case of three
360 and four TRM layers. When one or two TRM layers were used, the failure was attributed to
361 the concentration of the damage in one single crack. For this reason it is believed by the
362 authors that the concrete strength would not influence the results of specimens with one and
363 two TRM layers.

364 A comparison of the ultimate loads between the LX_N_Ls specimens (lower
365 compressive strength – approximately 15 MPa) and the LX_N specimens (higher
366 compressive strength – approximately 30 MPa) is made in Fig. 15c, d. In all cases, the use of
367 a lower compressive strength concrete had a negative impact on the load-carrying capacity of
368 the specimens. For specimens with lower concrete strength, the reduction in the ultimate
369 bond capacity was 4.1%, 12.5% and 3.1% for three TRM layers and 8%, 7.4% and 9.2% four
370 TRM layers, and for bond lengths equal to 100, 150, and 200 mm, respectively. As expected,
371 the lower (by 50%) compressive strength resulted in a decrease in the ultimate load which on
372 average was equal to approximately 7.5%. This reduction, though, cannot be considered as
373 significant as it may be in the range of the statistical error. It is noted that the insignificant

374 effect of the concrete strength on the load capacity has also been reported by D'Antino et al.
375 2015 [25]. However, in their study the concrete was not directly involved in the failure mode
376 which was at the interface between the matrix and the fibers.

377 **4.4 Influence of coating**

378 Coating the textile fabric with epoxy resin was investigated only for specimens with one and
379 two TRM layers, to improve the failure mode (slippage of the fibers through the mortar)
380 observed in these specimens with uncoated textiles. According to the results, the effect of
381 coating was twofold: (a) change in the failure mode, and (b) significant increase of the load-
382 carrying capacity. The failure mode changed from slippage of the fibers through the
383 surrounding matrix to debonding of TRM at the textile/mortar interface (interlaminar
384 shearing). Comparison of the ultimate loads of specimens with one and two layers of coated
385 textiles and of specimens with uncoated textiles is shown in Fig. 15e for different bond
386 lengths. The ultimate load was increased by 79.5% and 71.9% for specimens with one layer
387 and 16.6% and 13.5% for specimens with two layers, for bond lengths equal to 150 and 200
388 mm, respectively.

389 Coating the textile with epoxy resin makes the textile more stable and easy-to-apply,
390 while at the same time it increases its rigidity. When a good level of impregnation of the
391 fibers with resin is achieved, the inner filaments of the rovings are better bound to the outer
392 filaments. As a result, the mechanism of transferring stresses from the fibers to the matrix is
393 improved providing better mechanical interlock conditions. Ultimately, the textile fibers are
394 better utilized in carrying tensile forces and the load capacity increases. A more uniform
395 distribution of stresses is also achieved (something that is indicated by the formation of
396 several transversal cracks) and the failure mode changes from local slippage of the fibers to
397 global debonding of the TRM strips with the failure surface though being within the TRM
398 thickness (textile/mortar interface).

399 **4.5 Influence of anchorage through wrapping**

400 The influence of anchorage through confinement (full wrapping) was investigated for a short
401 bond length (100 mm) and for 3 and 4 TRM layers. The idea behind this was to improve the
402 bond conditions when a short bond length (less than the effective bond length) is provided, by
403 preventing early TRM debonding. As shown in Fig. 15f, the load capacity was increased by
404 28% and 45% when three and four TRM layers, respectively were anchored through
405 wrapping with TRM jackets; note that the bond length was equal to 100 mm whereas two
406 TRM layers were used for wrapping. As expected, the failure mode changed from TRM
407 debonding to partial rupture and slippage of the fibers across a single crack developed at the
408 loaded end (Fig. 12b).

409 A conclusion that must be highlighted is that the anchored TRM strips with a short
410 bond length (100 mm) not only reached, but exceeded the load capacity of non-anchored
411 strips with much higher bond length. Particularly, by comparing specimen L100_3_W with
412 specimens L200_3 and L250_3, an increase of the maximum load of 11.1% and 5.2%,
413 respectively, is observed. Similarly, by comparing specimen L100_4_W with specimens
414 L200_4 and L250_4, the increase in the maximum load reaches 22.3% and 21.4%,
415 respectively. Therefore, wrapping with TRM jackets is recommended to improve the bond
416 conditions when the available length for anchorage of TRM reinforcement is limited.

417 **5. Conclusions**

418 The present paper builds on the results of a comprehensive experimental programme for the
419 investigation of the bond between textile-reinforced mortar (TRM) and concrete. Eighty
420 specimens were fabricated and tested under double-lap shear. This poly-parametric study
421 included the investigation of: (a) the TRM bond length, (b) the number of TRM layers, (c) the
422 concrete surface preparation, (d) the concrete compressive strength, (e) the coating of the

423 textile, and (f) the anchorage through wrapping. The main conclusions drawn are summarized
424 below:

- 425 • By increasing the bond length, the bond capacity increases in a non-proportional way for
426 all the number of TRM layers examined (1 to 4). After a certain bond length, the so-called
427 effective bond length, the bond capacity marginally increases. It was found that this length
428 is in the range of 200-300 mm for the examined number of layers and for the materials
429 used in this study.
- 430 • By increasing the number of TRM layers for the same bond length, the bond capacity
431 increases in a non-proportional way. The increase was more pronounced for the transition
432 from one to two layers, whereas for more layers it was gradually becoming less
433 significant.
- 434 • The number of layers has a significant effect on the failure mode. For one and two TRM
435 layers the failure was due to slippage of the textile fibers through the mortar at a single
436 crack close to the loaded end. For three and four TRM layers the failure was attributed to
437 debonding at the mortar/concrete interface including detachment of a thin concrete layer,
438 similarly to EB FRP systems.
- 439 • Different concrete surface preparation methods (grinding and formation of a grid of
440 grooves versus sandblasting) did not influence the bond characteristic between TRM and
441 concrete, suggesting that both methods are suitable.
- 442 • The use lower concrete compressive strength marginally affected the bond strength of the
443 TRM to concrete. A 50% reduction in concrete's compressive strength resulted in an
444 average decrease of the ultimate bond capacity of 7.5%, without affecting the failure
445 mode.

- 446 • Coating the textile with an epoxy adhesive has a twofold effect: (a) change in the failure
447 mode from slippage through the mortar to TRM debonding at textile/mortar interface, and
448 (b) bond strength increase.
- 449 • The anchorage of TRM strips through wrapping with TRM jackets results in substantial
450 increase of the bond strength (up to 45% for 4 TRM layers), by preventing debonding
451 from the concrete substrate.

452 It is important to note that the above conclusions are based only on the materials used in this
453 study (specific carbon-fiber textile, and specific type of mortar). Therefore future research
454 could be directed towards investigating different types of materials, and deriving analytical
455 expressions for the calculation of the bond length and the bond strength of TRM composites
456 bonded to concrete surfaces.

457

458 **Acknowledgments**

459 The authors wish thank the technical staff Tom Buss, Mike Langford, Nigel Rook, Bal Loyla,
460 Gary Davies, Sam Cook and the PhD candidate Zoi Tetta, at the University of Nottingham
461 for their assistance to the experimental work. The research described in this paper has been
462 co-financed by the Higher Committee for Education Development in Iraq (HCED) and the
463 UK Engineering and Physical Sciences Research Council (EP/L50502X/1).

464 **References**

- 465 [1] Triantafillou TC, Papanicolaou CG, Zissimopoulos P, Laourdekis T. Concrete
466 confinement with textile-reinforced mortar jackets. *ACI Struct J* 2006;103(1):28-37.
- 467 [2] Bournas DA, Lontou PV, Papanicolaou CG, Triantafillou TC. Textile-reinforced mortar
468 versus fiber-reinforced polymer confinement in reinforced concrete columns. *ACI*
469 *Struct J* 2007;104(6).
- 470 [3] Carloni, C., Bournas, D. A., Carozzi, F.G., D'Antino, T., Fava, G., Focacci, F.,
471 Giacomini, G., Mantegazza, G., Pellegrino, C., Perinelli, C., and Poggi C., (2015).
472 "Fiber reinforced composites with cementitious (inorganic) matrix", Chapter 9 in:
473 Design procedures for the use of composites in strengthening of reinforced concrete
474 structures – State of the art report of the RILEM TC 234-DUC, (Eds: C. Pellegrino and
475 J. Sena-Cruz), pp. 349-391, Springer, RILEM STAR Book Series.
- 476 [4] Brückner A, Ortlepp R, Curbach M. Textile reinforced concrete for strengthening in
477 bending and shear. *Mater and struct* 2006;39(8):741-748.
- 478 [5] D' Ambrisi, A., and Focacci, F. Flexural strengthening of RC beams with cement-
479 based composites. *J Comp Constr* 2011; 15(5): 707-720.
- 480 [6] Loreto, G., Leardini, L., Arboleda, D., and Nanni, A. Performance of RC slab-type
481 elements strengthened with fabric-reinforced cementitious-matrix composites. *J Comp*
482 *Constr* 2013;18(3):10.1061/(ASCE)CC.1943-5614.0000415, 2014. A4013003.
- 483 [7] Koutas LN, Bournas DA. Flexural strengthening of two-way RC slabs with textile-
484 reinforced mortar: experimental investigation and design equations. *J Compos Constr*
485 2016. DOI: 10.1061/(ASCE)CC.1943-5614.0000713
- 486 [8] Azam R, Soudki K. FRCM strengthening of shear-critical RC beams. *J Comp Constr*
487 2014;18(5), 04014012. doi: 10.1061/(ASCE)CC.1943-5614.0000464.
- 488

- 489 [9] Tzoura, E, Triantafillou TC. Shear strengthening of reinforced concrete T-beams under
490 cyclic loading with TRM or FRP jackets. *Mater Struct* 2014;doi: 10.1617/s11527-014-
491 0470-9.
- 492 [10] Tetta, ZC., Koutas LN, and Bournas DA, Textile-reinforced mortar (TRM) versus
493 fiber-reinforced polymers (FRP) in shear strengthening of concrete beams. *Comps*
494 *Part B* 2015;77:338-348.
- 495 [11] Tetta, ZC, Koutas LN, and Bournas DA, Shear strengthening of full-scale RC T-
496 beams using textile-reinforced mortar and textile-based anchors. *Comps Part B*
497 2016;95:225-239.
- 498 [12] Ombres, L., and Verre S. Structural behaviour of fabric-reinforced cementitious
499 matrix (FRCM) strengthened concrete columns under eccentric loading. *Compo Part*
500 *B* 2015;75; 235-249.
- 501 [13] Bournas DA, Triantafillou TC, Zygouris K, Stavropoulos F. Textile-reinforced mortar
502 versus FRP jacketing in seismic retrofitting of RC columns with continuous or lap-
503 spliced deformed bars. *J Compos for Constr* 2009;13(5):360-371.
- 504 [14] Bournas DA, Triantafillou TC. Bond strength of lap-spliced bars in concrete confined
505 with composite jackets. *J Comp Constr* 2011;15(2):156-167.
- 506 [15] Bournas, D.A., and Triantafillou, T.C., (2011). "Bar Buckling in RC Columns Confined
507 with Composite Materials", *ASCE Journal of Composites for Construction*, 15(3), 393-
508 403.
- 509 [16] Bournas, D.A., and Triantafillou, T.C., (2013). "Biaxial Bending of RC Columns
510 Strengthened with Externally Applied Reinforcement Combined with Confinement",
511 *ACI Structural Journal*, 110(2), 193-204.
- 512 [17] Koutas L, Bousias SN, Triantafillou TC. Seismic strengthening of masonry-infilled RC
513 frames with TRM: Experimental study. *J Comp Constr* 2015;19(2):04014048. doi:
514 10.1061/(ASCE)CC.1943-5614.0000507.

- 515 [18] Papanicolaou CG., Triantafillou TC., Karlos K., Papathanasiou M. Textile reinforced
516 mortar (TRM) versus FRP as strengthening material of URM walls: out-of-plane cyclic
517 loading, *Mater and Struct* 2007; 41(1): 143-157.
- 518 [19] Faella C., Martinelli E., Nigro E, Paciello S. Shear capacity of masonry walls externally
519 strengthened by a cement-based composite material: An experimental campaign. *Constr*
520 *and Build Mat* 2010; 24 (1): 84-93.
- 521 [20] D'Ambrisi A, Feo L, Focacci F. Experimental analysis on bond between PBO-FRCM
522 strengthening materials and concrete. *Compos Part B* 2013; 44(1):524-532.
- 523 [21] D'Antino T, Pellegrino C, Carloni C, Sneed LH, Giacomini G. Experimental analysis
524 of the bond behavior of glass, carbon, and steel FRCM composites. In *Key Eng Mat*
525 2014;624:371-378.
- 526 [22] Sneed, L.H., T. D'Antino, and C. Carloni, Investigation of Bond Behavior of PBO
527 Fiber-Reinforced Cementitious Matrix Composite-Concrete Interface. *ACI Mater J*
528 2014; 111(1-6).
- 529 [23] Tran CT, Stitmannathum B, Ueda T. Investigation of the bond behaviour between
530 PBO-FRCM strengthening material and concrete. *J Adva Conc Tech*
531 2014;12(12):545-57.
- 532 [24] Awani O, El Refai A, El-Maaddawy T. Bond characteristics of carbon fabric-
533 reinforced cementitious matrix in double shear tests. *Constr and Build Mat*
534 2015;101:39-49.
- 535 [25] D'Antino T, Sneed LH, Carloni C, Pellegrino C. Influence of the substrate
536 characteristics on the bond behavior of PBO FRCM-concrete joints. *Constr and Build*
537 *Mat* 2015;30;101:838-850.
- 538 [26] Ombres L. Analysis of the bond between Fabric Reinforced Cementitious Mortar
539 (FRCM) strengthening systems and concrete. *Compos Part B* 2015;28;69:418-26.

- 540 [27] Sneed L.H., D' Antino T., Carloni C., and Pellegrino C., A comparison of the bond
541 behavior of PBO-FRCM composites determined by double-lap and single-lap shear
542 tests. *Cem and Conc Compos* 2015;64:37-48.
- 543 [28] EN 1015-11. Methods of test for mortar for masonry – Part 11: Determination of
544 flexural and compressive strength of hardened mortar, Brussels: Comité Européen de
545 Normalisation; 1993.
- 546 [29] Serbescu A, Guadagnini M, Pilakoutas K., Standardised double-shear test for
547 determining bond of FRP to concrete and corresponding model development. *Compos*
548 *Part B* 2013;55:277–297.
- 549 [30] Raof, S. M. Flexural strengthening of reinforced concrete beams with textile
550 reinforced mortar (TRM). PhD annual report (2nd year), Department of Civil
551 Engineering, The University of Nottingham: 2015.
- 552 [31] Yao, J., J. Teng, and J. Chen, Experimental study on FRP-to-concrete bonded joints.
553 *Compos Part B* 2005;36(2):99-113.
- 554

555 **Table 1** Specimens details, concrete compressive strength, and mortar properties on the day
 556 of testing

Specimen notation	Specimens name	Bond length (mm)	Number of TRM layers	Additional remarks	Concrete		Mortar				
					Compressive strength (MPa)*	Flexural strength (MPa)*	Compressive strength (MPa)*				
LX_N	L50_1 L50_2 L50_3 L50_4	50	1, 2, 3, 4	-	31.2 (0.56)	9.17 (0.92)	38.8 (0.60)				
	L100_1 L100_2 L100_3 L100_4	100	1, 2, 3, 4	-	30.4 (0.63)	8.24 (0.94)	33.8 (0.56)				
	L150_1 L150_2 L150_3 L150_4	150	1, 2, 3, 4	-	31.2 (0.22)	9.23 (0.49)	39.7 (1.33)				
	L200_1 L200_2 L200_3 L200_4	200	1, 2, 3, 4	-	32.8 (0.66)	8.54 (1.26)	35.9 (0.27)				
	L250_1 L250_2 L250_3 L250_4	250	1, 2, 3, 4	-	32.5 (0.32)	8.95 (0.37)	37.6 (0.90)				
	L450_1 L450_2	450	1, 2	-	29.5 (0.37)	9.4 (0.81)	40.1 (1.23)				
	LX_N_S	L100_3_S L100_4_S L150_3_S L150_4_S L200_3_S L200_4_S	100, 150, 200	3, 4	S= Surface preparation	29.3 (0.73)	8.68 (0.77)	36.8 (0.45)			
		LX_N_Ls	L100_3_Ls L100_4_Ls L150_3_Ls L150_4_Ls L200_3_Ls L200_4_Ls	100, 150, 200	3, 4	Ls= Low concrete strength	14.7 (0.55)	8.98	35.2 (0.90)		
			LX_N_C	L150_1_C L150_2_C L200_1_C L200_2_C	150, 200	1, 2	C= Textile coating	30.4 (0.28)	8.35 (0.65)	32.7 (0.97)	
				LX_N_W	L100_3_W L100_4_W	100	3, 4	W= Anchorage through wrapping with TRM		8.35 (0.65)	32.7 (0.97)

557 *Standard deviation in parenthesis

558

559 **Table 2** Summary of test results

Specimen	(1) Maximum load, P_{max} (kN)		(2) Displacement at maximum load δ_{max} (mm)		(3) Average maximum load, P_{av} (kN)	(4) Average displacement at maximum load δ_{av} (mm)	(5) Axial stress in textile fibers σ_t (MPa)	(6) Failure mode**
	S1*	S2*	S1*	S2*				
	L50_1	7.15	8.29	0.25	0.23	7.7	0.24	507
L50_2	19.12	17.76	0.79	0.70	18.4	0.75	605	a
L50_3	23.95	21.16	0.72	0.66	22.6	0.69	496	b
L50_4	26.46	29.31	0.46	0.62	27.9	0.54	459	b
L100_1	12.28	10.96	0.53	0.50	11.6	0.52	763	a
L100_2	22.82	24.14	1.01	1.00	23.5	1.01	773	a
L100_3	29.62	32.82	0.85	1.04	31.2	0.95	684	b
L100_4	32.77	37.27	0.83	0.92	35.0	0.88	576	b
L150_1	11.74	12.58	1.32	1.21	12.2	1.27	803	a
L150_2	25.25	25.34	1.10	1.11	25.3	1.11	832	a
L150_3	34.49	35.62	1.05	1.07	35.1	1.06	770	b
L150_4	38.55	37.2	1.4	1.51	37.9	1.46	623	b
L200_1	13.51	14.25	1.23	1.24	13.9	1.24	915	a
L200_2	27.65	28.59	1.35	0.81	28.1	1.08	924	a
L200_3	37.44	34.55	1.56	1.9	36.0	1.73	790	b
L200_4	41.26	41.74	1.31	1.57	41.5	1.44	683	b
L250_1	14.92	17.32	2.29	2.55	16.1	2.42	1059	a
L250_2	30.25	28.63	1.2	1.6	29.4	1.40	967	a
L250_3	38.55	37.51	1.56	1.55	38.03	1.56	834	b
L250_4	42.79	40.89	1.22	1.35	41.8	1.29	688	b
L450-1	17.54	17.2	2.51	2.15	17.4	2.33	1145	a
L450-2	32.8	30.4	3.51	3.62	31.6	3.57	1040	a
L100_3_S	30.64	31.77	1.27	1.46	31.2	1.37	684	
L150_3_S	34.99	32.74	0.99	1.05	33.9	1.02	743	
L200_3_S	40.18	40.57	1.85	1.19	40.4	1.52	886	
L100_4_S	35.63	36.58	1.24	0.75	36.1	1.00	594	b
L150_4_S	37.64	36.74	1.19	0.80	37.2	1.00	612	
L200_4_S	41.45	42.35	1.35	1.19	41.9	1.27	689	
L100_3_Ls	29.9	29.84	1.04	1.12	29.9	1.08	656	
L150_3_Ls	30.67	30.79	1.36	1.29	30.7	1.33	673	
L200_3_Ls	33.68	36.17	1.81	1.99	34.9	1.90	765	
L100_4_Ls	32.67	31.76	0.92	0.85	32.2	0.89	530	b
L150_4_Ls	34.7	35.54	1.13	1.45	35.1	1.29	577	
L200_4_Ls	36.81	38.63	1.48	1.39	37.7	1.44	620	
L150_1_C	22.7	21.08	1.45	1.64	21.9	1.55	1441	
L200_1_C	23.21	24.6	1.44	1.54	23.9	1.49	1572	
L150_2_C	29.1	29.89	0.8	0.89	29.5	0.85	970	c
L200_2_C	32.94	30.77	0.95	1.05	31.9	1.00	1049	
L100_3_W	38.43	41.47	1.21	1.29	40.0	1.25	877	
L100_4_W	49.19	52.31	1.17	1.25	50.75	1.21	835	a

* Specimen number

** a: Slippage and partial rupture of textile fibers through the mortar; b: Debonding of TRM from the concrete substrate including part of the concrete cover; c: Debonding at the textile/mortar interface (interlaminar shearing)

560
561
562
563

564 **Table 3** Percentage of the residual load due to friction with respect to maximum recorded
 565 load for specimens with one and two layers of TRM

566

Name	Percentage of residual load (%)	
	S1*	S2*
L50_1	36.4	36.2
L50_2	33.5	28.5
L100_1	46.9	57.8
L100_2	33.3	34.0
L150_1	60.7	60.1
L150_2	46.6	43.4
L200_1	57.0	61.1
L200_2	56.8	65.8
L250_1	42.2	61.2
L250_2	52.2	52.4
L450-1	71.3	70.3
L450-2	75.0	81.6

567

568

* Specimen number

569

570

571

572

573

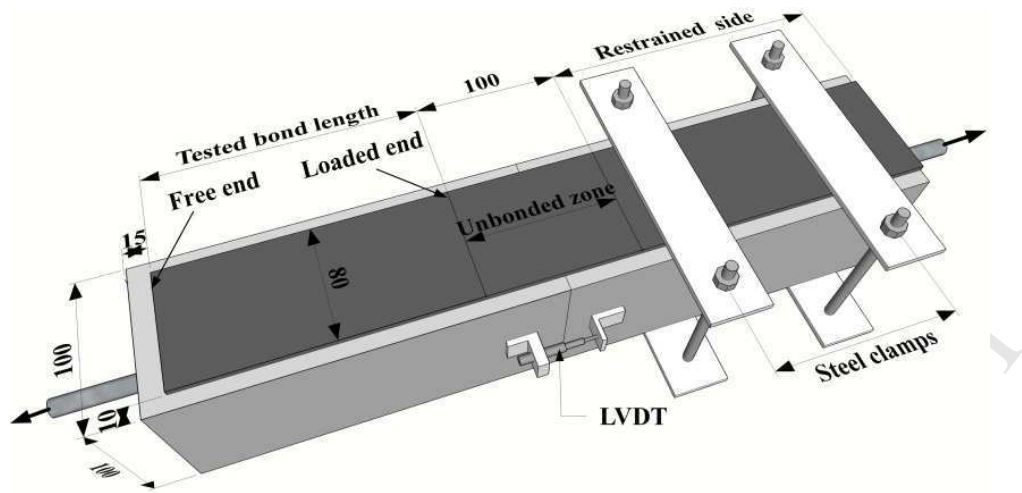
574

575

576

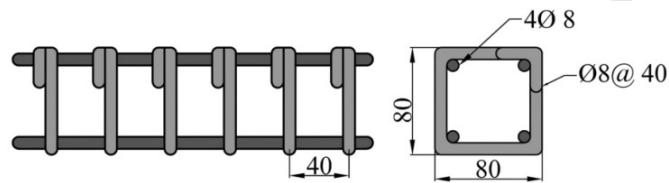
577

578



579

(a)



580

(b)

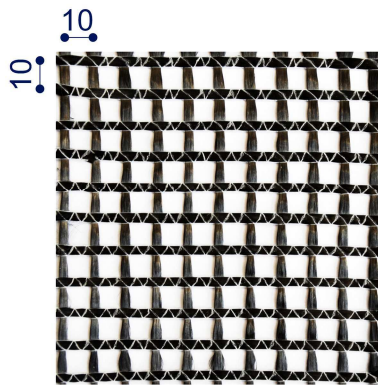
581

Fig. 1 Specimen details (dimensions in mm)

582

583

584



585

586

Fig. 2 Carbon textile used in this study (dimensions in mm)



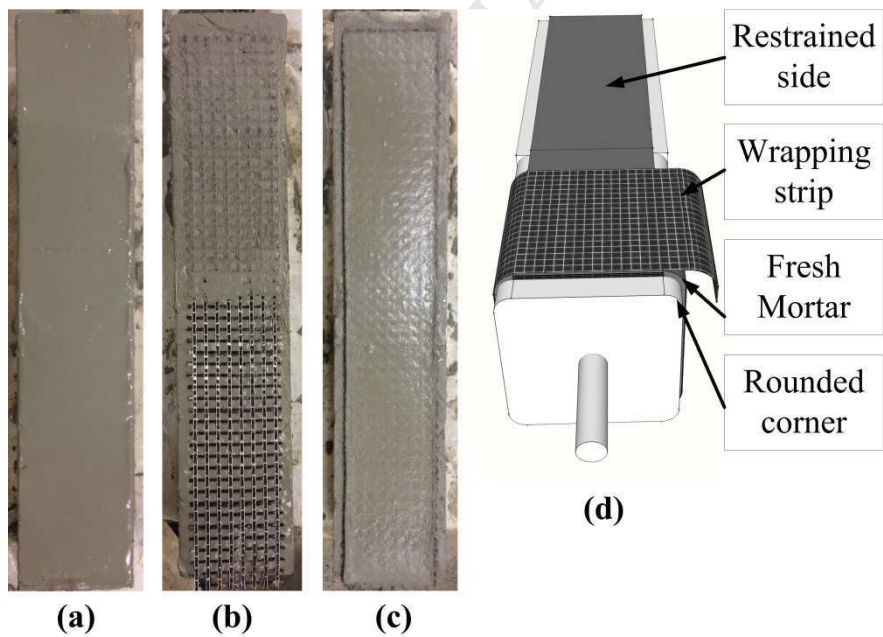
587

588 **Fig. 3** Different concrete surface preparation: (a) grinding and creating a grid of grooves;
589 and (b) sandblasting

590

591

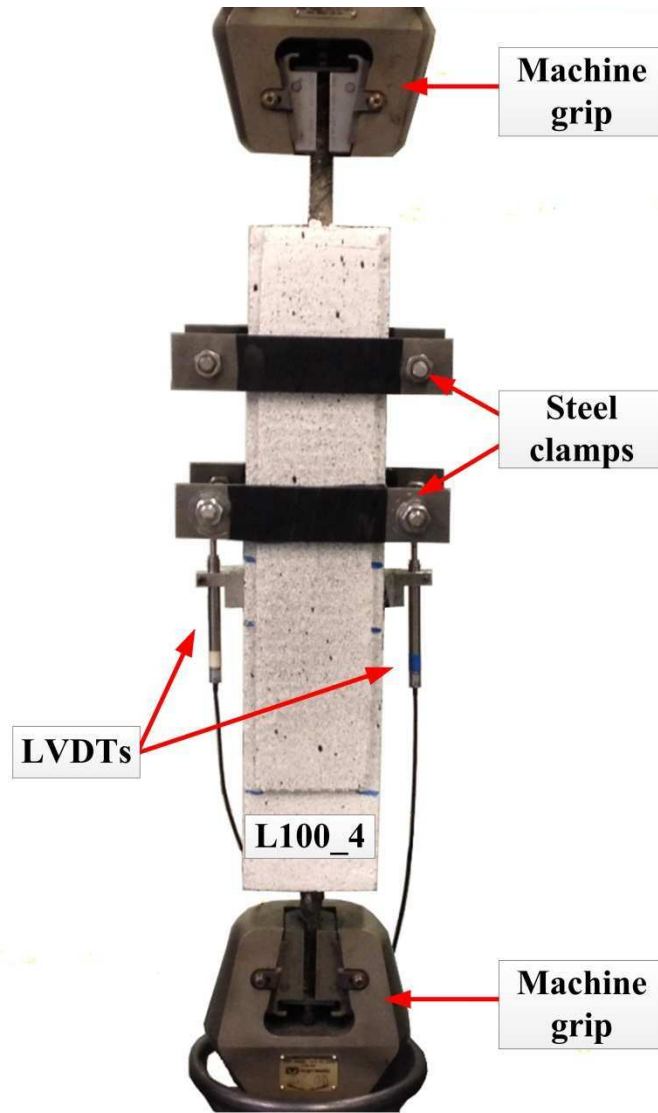
592



593

594 **Fig. 4** (a) Application of the first layer of mortar; (b) application of the first layer of textile
595 layer into the mortar; (c) application of the final layer of mortar; and (d) wrapping
596 with TRM jacket at the side of specimen under examination.

597



598

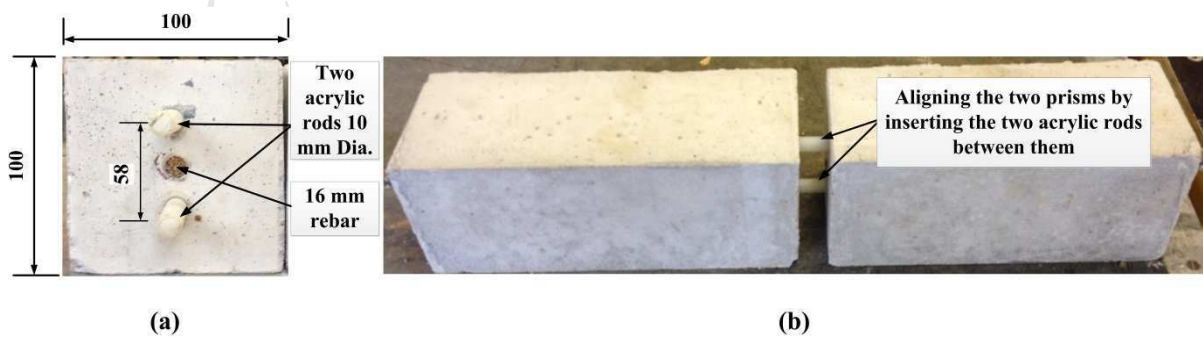
599

600

601

602

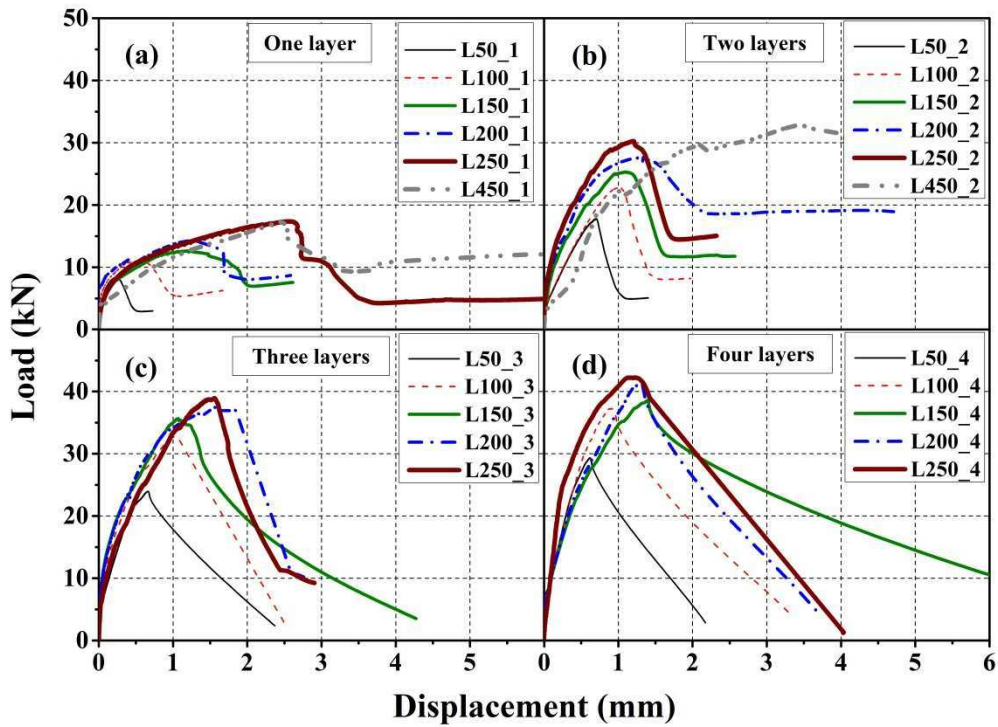
Fig. 5 Details of the test set-up



603

604

Fig. 6 Alignment of the two concrete prisms using two acrylic rods (Dimensions in mm)



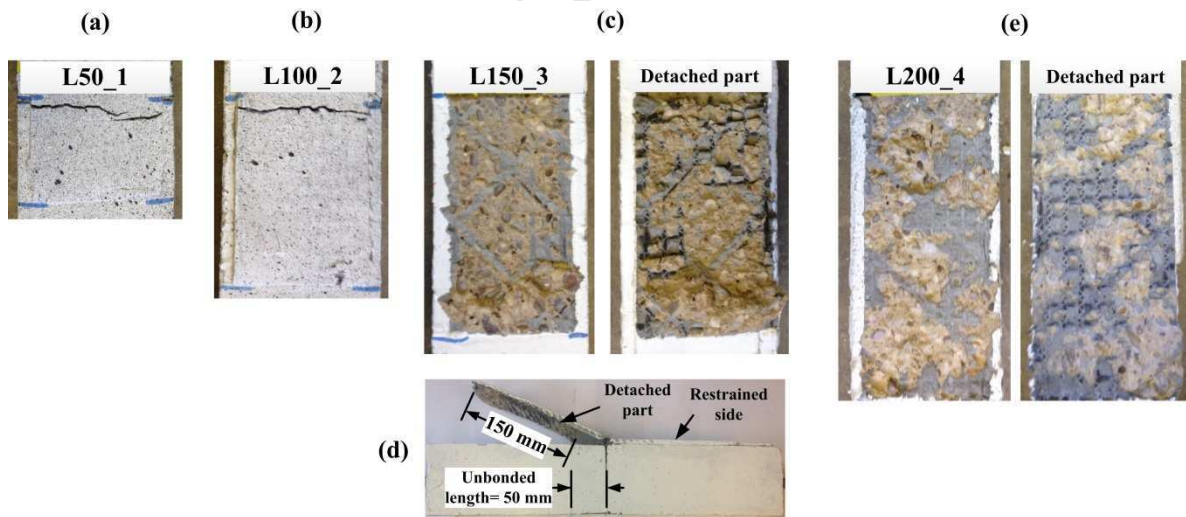
605

606

Fig. 7 Load-displacement curves of LX_N group specimens

607

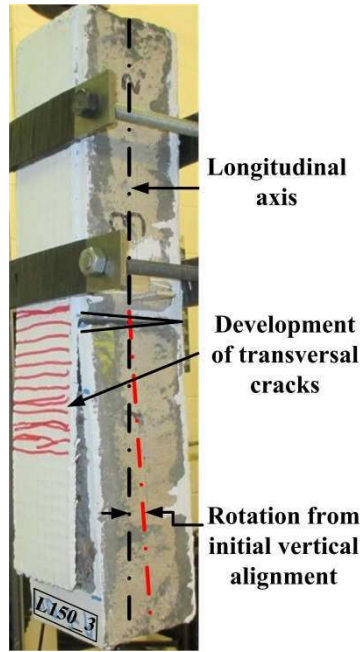
608



609

Fig. 8 Failure mode of specimens in group LX_N: (a),(b) single crack formation and slippage of the fibers through the mortar for specimens with one and two TRM layers, respectively; (c),(d),(e) TRM debonding at concrete/matrix interface including a thin layer of concrete cover, for specimens with three and four layer.

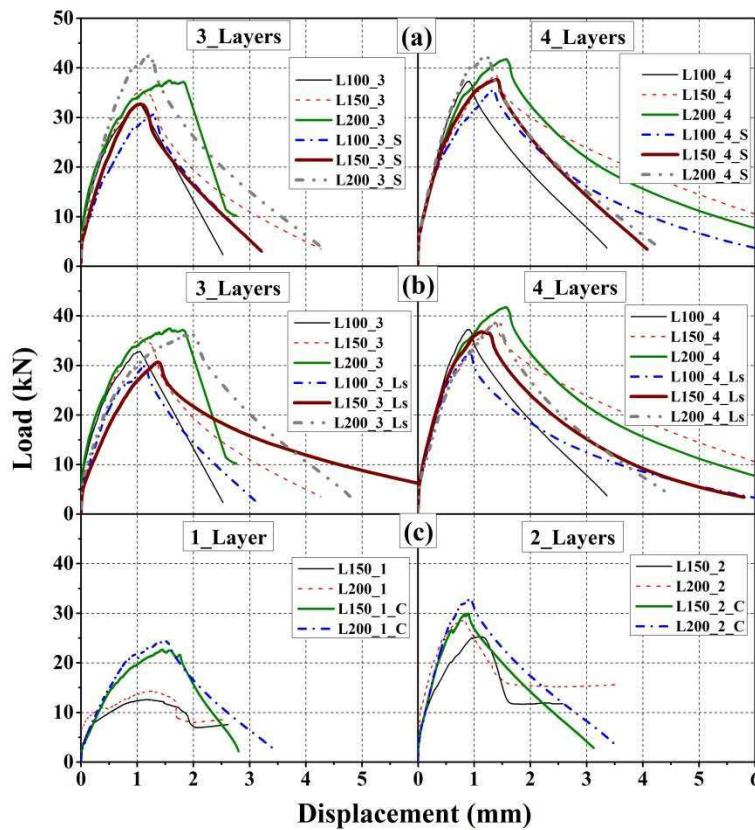
614



615

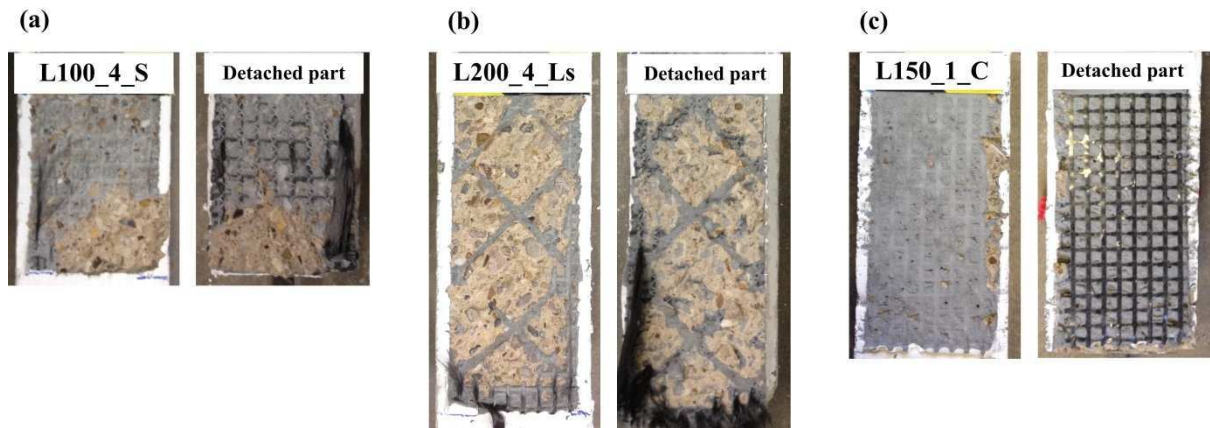
616 **Fig. 9** Development of transversal cracks and the rotation of the specimen relative to initial
 617 alignment after ultimate load

618



619

620 **Fig. 10** Load-displacement curves for specimens having as a parameter; (a) the concrete
 621 surface preparation, (b) the concrete compressive strength and (c) the textile coating



622

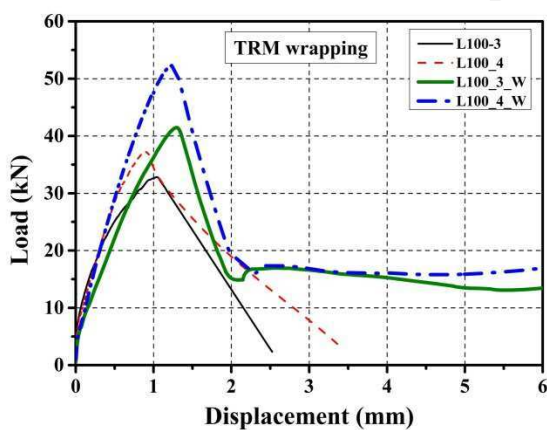
623

624 **Fig. 11** Typical failure mode of specimens with: (a) sandblasted concrete surface, (b) low
 625 concrete compressive strength, and (c) coated textiles

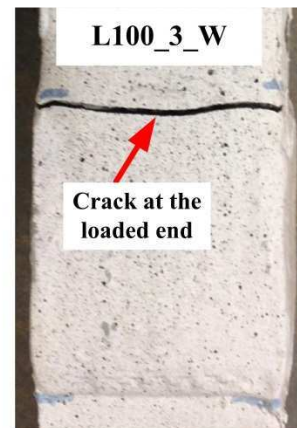
626

627

628



(a)



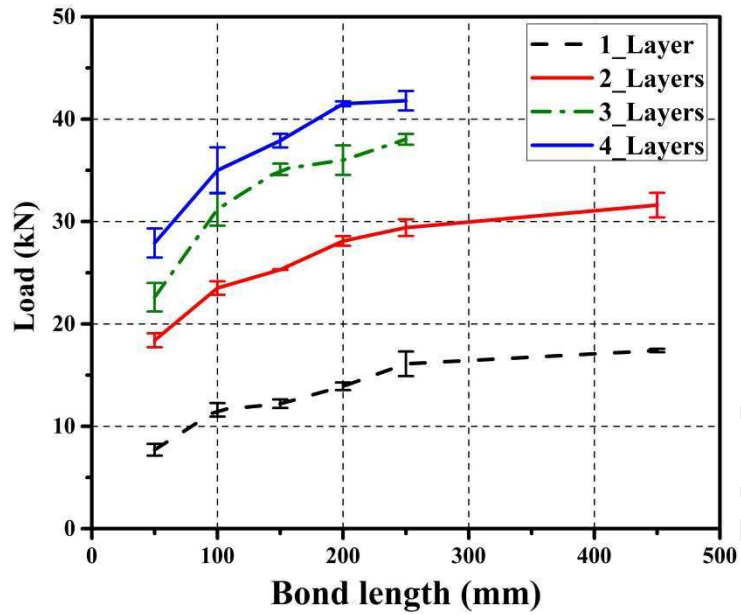
(b)

629

630 **Fig. 12** (a) Load-displacement curves of specimens with anchorage through wrapping and

631 comparison with counterpart specimens without anchorage; (b) typical failure of specimens

632 with anchorage through wrapping with TRM jackets



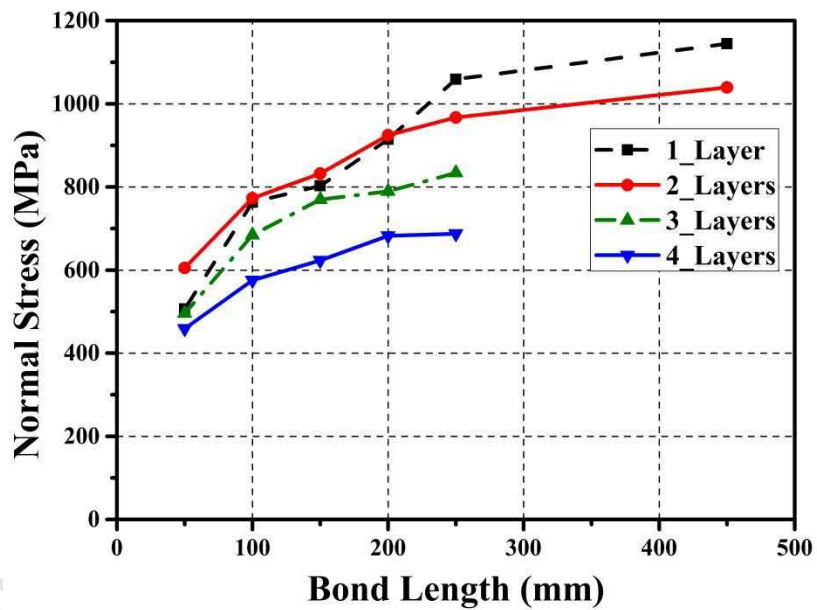
633

634

Fig. 13 Variation of ultimate load with the number of layers and bond length

635

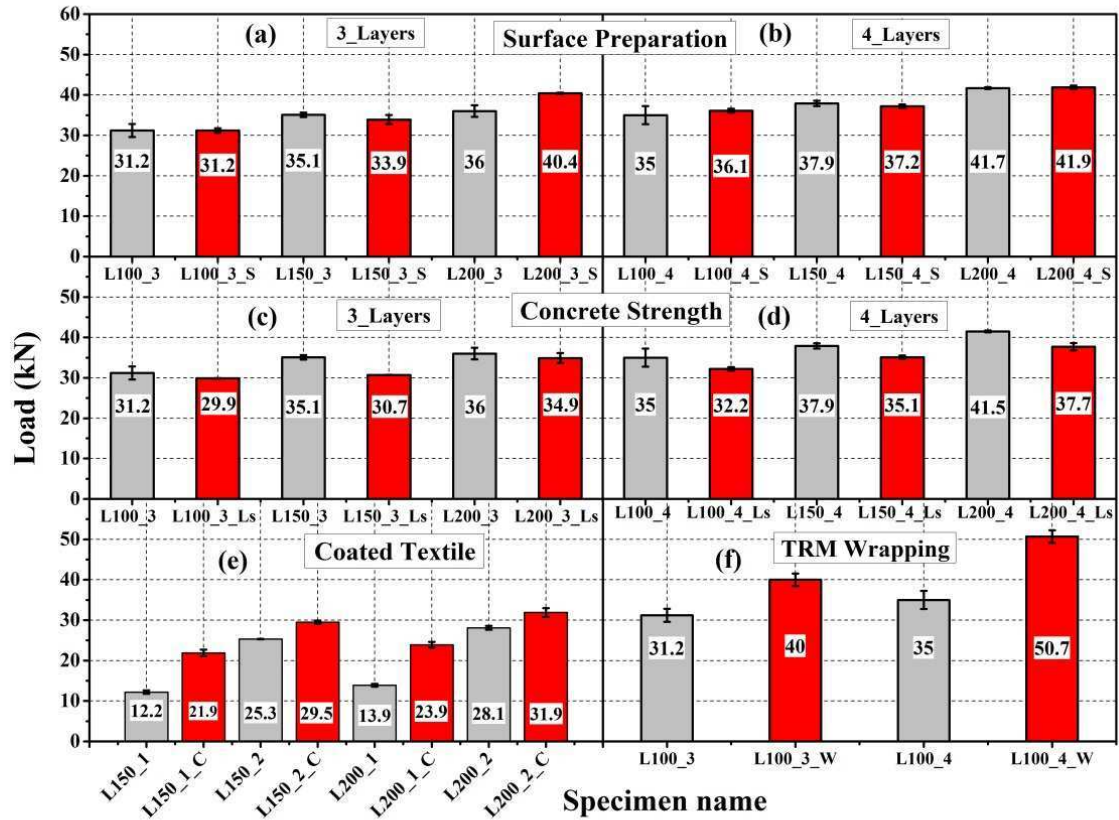
636



637

638

Fig. 14 Variation of normal stress with the number of layers and bond length



639

640

641 **Fig. 15** Effect of different parameters on the bond capacity of the specimens: (a), (b) surface
 642 preparation; (c),(d) concrete compressive strength; (e) textile coating; (f) anchorage
 643 through wrapping with TRM jackets